Full Canonical Information from Grand-Potential Density-Functional Theory

Daniel de las Heras and Matthias Schmidt*
Theoretische Physik II, Physikalisches Institut, Universität Bayreuth, D-95440 Bayreuth, Germany
(Received 17 September 2014; published 5 December 2014)

We present a general and formally exact method to obtain the canonical one-body density distribution and the canonical free energy from direct decomposition of classical density functional results in the grand ensemble. We test the method for confined one-dimensional hard-core particles for which the exact grand potential density functional is explicitly known. The results agree to within high accuracy with those from exact methods and our Monte Carlo many-body simulations. The method is relevant for treating finite systems and for dynamical density functional theory.

DOI: 10.1103/PhysRevLett.113.238304 PACS numbers: 82.70.Dd, 05.70.-a, 71.15.Mb, 82.35.-x

Classical density functional theory (DFT) [1–3] forms an essential tool for the investigation of a broad spectrum of simple [4] and complex systems [5] in soft condensed matter. While DFT was shown to describe a broad range of the occurring phenomena, typically the investigated systems contain at least one large spatial dimension, such that a thermodynamic limit can be performed, where the volume $V \to \infty$ and the number of particles $N \to \infty$ upon keeping the mean particle density $N/V = \text{const}$.

Evans [1] and Mermin [3] originally formulated the exact variational principle of DFT using the grand ensemble, where N fluctuates and the chemical potential μ, the volume V, and the absolute temperature T constitute the independent thermodynamic variables. The equilibrium thermodynamic grand potential $\Omega_0(\mu, V, T)$ generalizes to a grand potential functional $\Omega([\rho], \mu, V, T)$ of the one-body density distribution $\rho(\mathbf{r})$, where $\mathbf{r}$ indicates position. Within the variational theory, $\rho(\mathbf{r})$ forms the trial field which is *a priori* unknown. For a given thermodynamic state at μ, V, and T it is the equilibrium grand canonical density distribution $\rho_0(\mathbf{r})$ which minimizes Ω [1,3]. Hence, at the minimum

$$\left.\frac{\delta\Omega([\rho], \mu, T, V)}{\delta\rho(\mathbf{r})}\right|_{\rho_0(\mathbf{r})} = 0. \tag{1}$$

Evaluating the functional at $\rho_0(\mathbf{r})$ yields the thermodynamic grand potential, $\Omega[\rho_0] = \Omega_0$.

Both ensembles, grand canonical and canonical, are equivalent in the thermodynamic limit and the differences between them can be negligible if $N \gtrsim 10^2$. Nevertheless, there are many interesting systems where the number of particles is small and the occurring structuring depends nontrivially on N. Examples are the confinement of hard spheres in spherical cavities [6], isolated colloidal clusters with $\sim$10 particles [7], spherical colloids confined in adaptive two-dimensional cavities [8], and the formation of domain walls in two-dimensional confined anisotropic particles [9].

Further interest in a canonical description originates from the highly successful dynamical DFT for Brownian dynamics [1,10]. Here the time evolution via the underlying Brownian many-body dynamics is intrinsically particle conserving, and should, hence, be more appropriately modeled canonically than, as is usually done, grand canonically.

Previous efforts to construct a canonical DFT were based, e.g., on adding a correction term to the grand potential functional [11] in order to suppress the density fluctuations. In Ref. [6], González *et al.* expressed the canonical density distribution via a series expansion in powers of the inverse average number of particles. By truncating the series, they could obtain rather accurate canonical profiles from grand canonical DFT in a system of confined hard spheres. The method was subsequently applied to a system of one-dimensional rods [12]. The formal extension of the DFT formalism to the canonical ensemble can be based on the Mermin-Evans argument [13] or on Levy's constrained search method [14].

In this Letter we present a general and formally exact method to obtain the canonical one-body density distribution and the canonical partition function using a given grand canonical density functional. The method is based on decomposing the smooth variation with μ of the grand canonical quantities into the underlying discrete, N-dependent canonical quantities. In order to demonstrate the validity of the method we consider the one-dimensional system of confined hard particles. As Percus' (grand) free energy functional for this system is exact, we obtain the exact canonical density profiles and the exact canonical partition functions for each discrete value of N.

In detail, we consider N one-dimensional hard rods of length σ confined between two parallel walls that are separated by a distance h. The interaction between a particle and each wall is also hard core; i.e., the particles cannot penetrate the walls. We compute the grand canonical density profiles $\rho_0(x;\mu)$, where x is the space variable, using the exact grand canonical density functional [15].

The minimization is performed using a standard conjugate gradient method (see, e.g., Ref. [16] for details about the implementation). As a reference we use benchmark results for canonical density profiles $\rho_N(x)$ from our canonical Monte Carlo (MC) simulations, where we first equilibrate the system by performing 10^6 MC steps and then run 10^8–10^{10} steps to obtain the density profiles.

In order to illustrate the differences between canonical and grand canonical ensembles we show, in Fig. 1, density profiles for a pore with $h/\sigma = 4.9$. The values of μ in the grand ensemble are chosen such that the resulting average total number $\bar{N}$ of particles equals their (integer) number N in the corresponding canonical system. In both grand canonical and canonical ensembles the number of particles can be calculated via the spatial integrals of the corresponding density profiles:

$$\bar{N}(\mu) = \int_V dx \rho_0(x;\mu), \tag{2}$$

$$N = \int_V dx \rho_N(x). \tag{3}$$

Because of the hard-core nature of the confined system, the maximal number of particles is $N_{\max} = 4$ for the chosen value of h. The density profiles in both ensembles are strikingly different from each other, as is exemplified by the

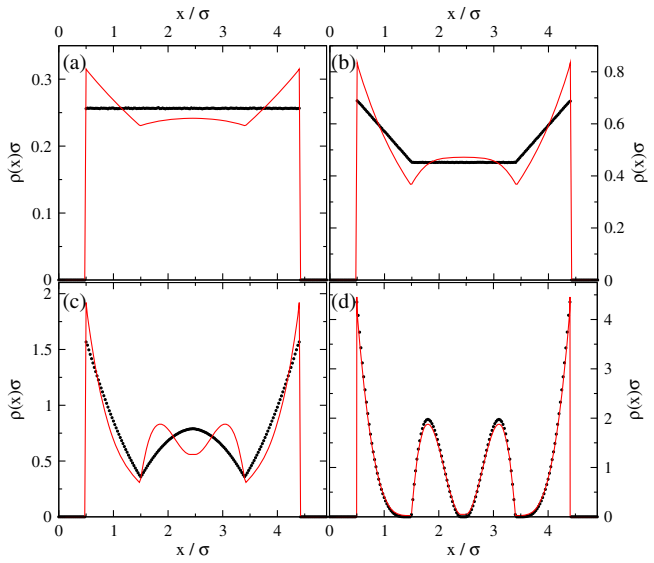

FIG. 1 (color online). Scaled density profiles $\rho(x)\sigma$ as a function of x/σ in the canonical ensemble (black symbols) and in the grand canonical ensemble (red lines) obtained with canonical MC simulation and the exact grand canonical DFT, respectively. The pore width is $h/\sigma = 4.9$. The canonical number of particles N equals the average grand canonical number of particles $\bar{N}$ in cases (a) $N = 1$; (b) $N = 2$; (c) $N = 3$. In (d) $N = 4$ and $\bar{N} \approx 3.95$. Note that $\bar{N} = 4$ corresponds to the limit $\mu \to \infty$ that cannot be achieved by numerical minimization of the functional.

canonical profile for $N = 1$, cf. Fig. 1(a), which is constant within the allowed region ($0.5\sigma \le x \le h - 0.5\sigma$). However, the corresponding grand canonical profile with $\bar{N} = 1$ exhibits clear structuring due to the combination of underlying canonical profiles.

First we describe how to obtain the canonical partition functions $Z_N(V,T)$ from the grand canonical DFT. The grand partition function of a given system is

$$\Xi(\mu,V,T) = \sum_{N=0}^{\infty} e^{\beta\mu N} Z_N(V,T), \tag{4}$$

where $\beta = 1/k_B T$, with k_B being the Boltzmann constant. Note that in a closed system of hard cores, such as the present one, the sum truncates at a maximal number of particles, $N_{\max}$. The thermodynamic grand potential is

$$\Omega_0(\mu,V,T) = -k_B T \ln \Xi(\mu,V,T). \tag{5}$$

Combining Eqs. (4) and (5), we find

$$\exp[-\beta\Omega_0(\mu,V,T)] - 1 = \sum_{N=1}^{\infty} e^{\beta\mu N} Z_N(V,T), \tag{6}$$

where the partition function of the empty state is $Z_0 = 1$ (which only affects the normalization of the grand canonical partition function, and therefore an unimportant additive constant in the grand potential). Equation (6) can be rewritten as

$$1 = \sum_{N=1}^{\infty} c_N(\mu,T,\Omega_0) Z_N, \tag{7}$$

with

$$c_N(\mu,T,\Omega_0) = \frac{\exp[\beta\mu N + \beta\Omega_0(\mu)]}{1 - \exp[\beta\Omega_0(\mu)]}, \tag{8}$$

where we have suppressed the dependence of Ω_0 and Z_N on V and T in the notation. Given a grand canonical DFT, minimizing the functional for given values of μ, V, and T yields results for $\Omega_0(\mu)$. This enables us to calculate the coefficients c_N for each N according to Eq. (8). By repeating the procedure for different values of μ we obtain a set of linear equations, cf. Eq. (7), where the only unknown variables are the canonical partition functions Z_N. Numerically, solving this set of linear equations yields results for the Z_N. In Fig. 2, we show the numerically obtained canonical partition functions for the one-dimensional system as a function of the wall separation h. We compare these results with the analytic expression for the partition function [17], $Z_N = ((h - N\sigma)/\Lambda)^N/N!$, where Λ is the (irrelevant) thermal wavelength that we have set as $\Lambda = \sigma$. The agreement is perfect.

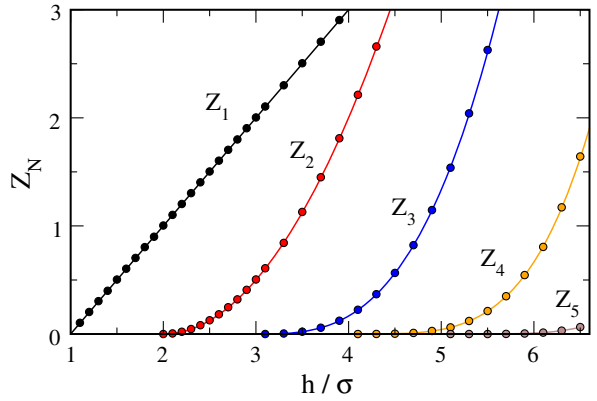

FIG. 2 (color online). Canonical partition functions Z_N for a range of particle numbers $N = 1$–5 (as indicated) of a system of one-dimensional hard particles confined between hard walls as a function of the scaled wall separation distance h/σ. The lines represent the analytic solution. The symbols indicate the numerical results for the partition functions obtained from decomposition of the exact grand canonical DFT results.

In order to further demonstrate the validity of the method, we have computed the equation of state $\bar{N}(\mu)$ using three different approaches: (i) minimizing the grand canonical DFT at different μ and obtaining $\bar{N}(\mu)$ as the space integral of the (grand canonical) density distribution, see Eq. (2), (ii) using the obtained results for Z_N to compute the grand canonical partition function via Eq. (4) and then using the thermodynamic relation

$$\bar{N}(\mu) = \left.\frac{\partial \ln \Xi}{\partial(\beta\mu)}\right|_{V,T}, \tag{9}$$

and (iii) as an average in the grand canonical ensemble

$$\bar{N}(\mu) = \sum_{N=0}^{\infty} p_N(\mu) N, \tag{10}$$

where

$$p_N(\mu) = \exp(\beta\mu N)\frac{Z_N}{\Xi(\mu)}, \tag{11}$$

is the probability of finding N particles at given value of μ. The results are shown in Fig. 3(a). The three curves lie on top of each other. In Figs. 3(b) and 3(c) we show the probabilities p_N as a function of μ and $\bar{N}$, respectively. As expected the probability of finding N particles is maximal at the value of the chemical potential for which $\bar{N}(\mu) = N$. At high values of μ almost only the state with four particles contributes to the grand canonical state because states with $N > 4$ are not allowed. Actually, in the limit $\mu \to \infty$ the grand canonical state with $\bar{N} = 4$ is the same as the canonical state with $N = 4$ [cf. Fig. 1(d)] in this pore. However, in wider pores differences between canonical and grand canonical ensembles can be observed at higher values of N.

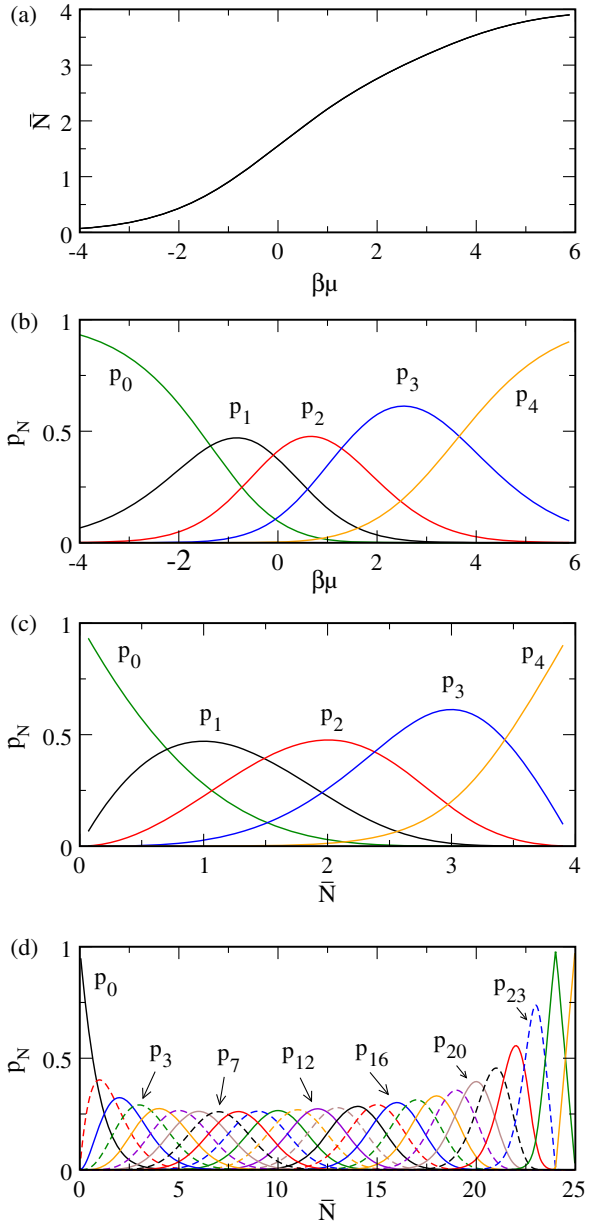

FIG. 3 (color online). (a) Average number of particles $\bar{N}$ as a function of the scaled chemical potential $\beta\mu$ in a pore with $h/\sigma = 4.9$ calculated with three different methods. The lines lie on top of each other. (b) Probability p_N of finding $N = 0$–4 (as indicated) particles in a pore with $h/\sigma = 4.9$ as a function of $\beta\mu$. (c) p_N as a function of the average number of particles $\bar{N}$ inside the pore. (d) p_N, with $N = 0$–25, as a function of $\bar{N}$ in a pore with $h/\sigma = 25.9$ and a parabolic external potential.

The method remains valid in the presence of an external potential. As an example, we show in Fig. 3(d) p_N as a function of $\bar{N}$ in a pore with $h/\sigma = 25.9$ and a parabolic external potential $\beta V_{\text{ext}}(x) = 0.05(x - h/2)^2\sigma^{-2}$.

Next we decompose the one-body grand canonical distribution function into one-body canonical distribution

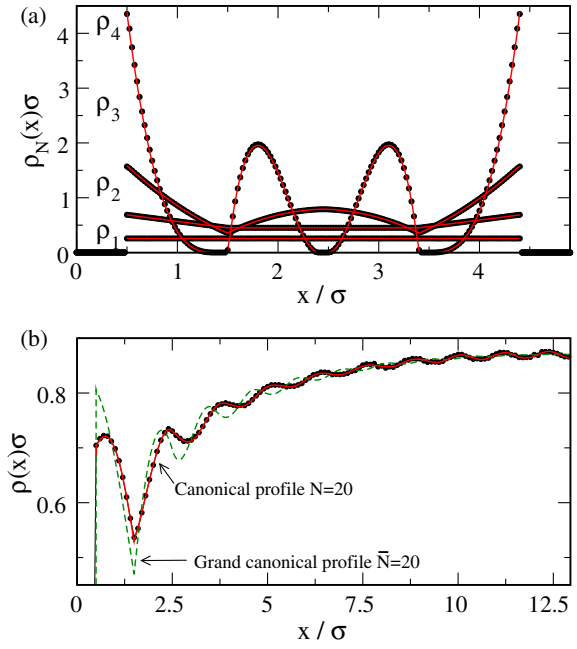

FIG. 4 (color online). Scaled canonical density profiles $\rho_N(x)\sigma$ obtained by MC simulation (black symbols) and using the grand canonical decomposition (red lines) of the exact grand canonical DFT for: (a) $N = 1$–4 in a pore with $h/\sigma = 4.9$, and (b) $N = 20$ in a pore with $h/\sigma = 25.9$ with a parabolic external potential $\beta V_{\text{ext}}(x) = 0.05(x - h/2)^2\sigma^{-2}$. The dashed green line in (b) is the grand canonical profile for $\bar{N} = 20$. Only the left half of the profiles are shown in (b).

functions. Using Eqs. (2), (3), and (10) allows us to express the grand canonical one-body distribution as a linear combination of canonical distributions:

$$\rho_0(x;\mu) = \sum_{N=0}^{\infty} p_N(\mu)\rho_N(x). \tag{12}$$

All terms in the above expression are known except for the canonical density profiles. Analogous to the case of the partition function above, these can be obtained by solving a set of linear equations, where the unknown quantities are the canonical profiles, $\rho_N(x)$. This procedure applies locally, i.e., for each value of x. The results are plotted in Fig. 4, where we compare with the canonical profiles obtained from MC simulations. The agreement is excellent and demonstrates that one indeed is able to decompose the grand canonical density profiles into the exact canonical density profiles. While in wide pores the differences between canonical and grand canonical profiles are small or even negligible at intermediate packing fractions, significant differences can be observed at high packing fractions, see Fig. 4(b) for an example case.

To summarize, we have developed a method to obtain the canonical partition functions and the canonical one-body density distributions, using a given grand canonical DFT. We have applied the method to a one-dimensional system of hard rods for which the exact grand canonical free energy functional is known. Therefore, the results for canonical partition functions and for the canonical density profiles are (numerically) exact. If one starts with an approximate grand ensemble free energy functional, the resulting canonical partition functions and profiles will be also approximative. Their accuracy will depend on the quality of the starting grand canonical DFT. Hence, the present method can also be used to test the accuracy of a grand canonical DFT by decomposition and comparing the resulting canonical profiles to those obtained in simulations (or experiments).

The set of linear equations that we have used to find the canonical partition sums, cf. Eq. (7), requires as an input the grand potential. Alternatively, we can combine Eqs. (4) and (10), resulting in

$$\sum_{N=0}^{\infty} e^{\beta\mu N}[N - \bar{N}(\mu)]Z_N = 0. \tag{13}$$

In order to find Z_N using Eq. (13) one only needs $\bar{N}$ as a function of μ. Thus, this might constitute a suitable method to obtain Z_N in grand canonical simulations (or experiments).

Furthermore, the direct decomposition method might be used to accelerate the numerical minimization of grand canonical DFT for finite systems as follows: (i) minimize the DFT for a given set of values of the chemical potential; (ii) obtain the canonical partition functions and density profiles; (iii) use Z_N and the canonical profiles to straightforwardly obtain the grand canonical potential and density profiles for any value of chemical potential. This decomposition-recomposition scheme might be also applied to obtain grand canonical states at very high chemical potential; this is a regime that is difficult to access by direct minimization of the functional. In order to decompose the functional one only needs a range in μ to which all the canonical states contribute. For example, in the pore with $h/\sigma = 4.9$, the range $0 \le \beta\mu \le 2$ [see Fig. 3(b)] is enough to find all the canonical partition sums and density profiles in the pore. Once these are known we can recompose the canonical profiles and obtain the limit $\mu \to \infty$ that corresponds to a pore with $N = 4$.

From a numerical point of view the decomposition scheme is a local, "postprocessing" routine, which does neither depend on the complexity of the functional nor on that of the external potential. It consists of solving a set of linear equations with $\sim N_{\max}$ unknowns (at each space point). Even for the simple functional used here, this procedure is therefore much faster than the DFT minimization routine. However, as the values of the coefficients c_N in Eq. (8) vary over many orders of magnitude, systems with $N_{\max} \gtrsim 50$ become increasingly difficult to treat with the standard solution methods that we use here. The use of higher than double precision numerics might alleviate this problem. An alternative, in particular for systems where

there is no restriction on the maximum number of particles, consists of truncating the coefficients c_N beyond a given value of N. This applies provided that the chemical potentials selected for the decomposition are such that the truncated coefficients are sufficiently small. However, care must be taken in order to not introduce truncation artifacts.

Besides the partition sum and one-body density profiles, the decomposition method applies to all further grand ensemble averages. This includes, in particular, canonical two-body correlation functions, to be obtained from the (usual) grand ensemble results (e.g., within DFT from the Ornstein-Zernike or test-particle routes, or, alternatively, from liquid state integral equation theories). The availability of such canonical results (for finite systems) offers the exciting possibility to shed further light on the canonical version of the Ornstein-Zernike equation, as developed by Ramshaw [18], Hernando, and Blum [14], and White and González [19]. Furthermore, our method offers the possibility to study ensemble differences in solvation phenomena [1]. We have stayed away from phase transitions where multiple solutions might occur.

*Matthias.Schmidt@uni-bayreuth.de

[1] R. Evans, Adv. Phys. **28**, 143 (1979).
[2] R. Evans, *Fundamentals of Inhomogeneous Fluids* (CRC Press, New York, 1992), pp. 85–175.
[3] N. D. Mermin, Phys. Rev. **137**, A1441 (1965).
[4] J. F. Lutsko, Adv. Chem. Phys. **144**, 1 (2010).
[5] J. Wu and Z. Li, Annu. Rev. Phys. Chem. **58**, 85 (2007).
[6] A. González, J. A. White, F. L. Román, S. Velasco, and R. Evans, Phys. Rev. Lett. **79**, 2466 (1997).
[7] G. Meng, N. Arkus, M. P. Brenner, and V. N. Manoharan, Science **327**, 560 (2010).
[8] I. Williams, E. C. Oguz, R. L. Jack, P. Bartlett, H. Löwen, and C. P. Royall, J. Chem. Phys. **140**, 104907 (2014).
[9] D. de las Heras and E. Velasco, Soft Matter **10**, 1758 (2014).
[10] U. M. B. Marconi and P. Tarazona, J. Chem. Phys. **110**, 8032 (1999).
[11] J. A. White, A. González, F. L. Román, and S. Velasco, Phys. Rev. Lett. **84**, 1220 (2000).
[12] S.-C. Kim, J. Chem. Phys. **110**, 12265 (1999).
[13] W. S. B. Dwandaru and M. Schmidt, Phys. Rev. E **83**, 061133 (2011).
[14] J. A. Hernando and L. Blum, J. Phys. Condens. Matter **13**, L577 (2001).
[15] J. K. Percus, J. Stat. Phys. **15**, 505 (1976).
[16] P. Tarazona, J. Cuesta, and Y. Martínez-Ratón, Lect. Notes Phys. **753**, 247 (2008).
[17] L. Tonks, Phys. Rev. **50**, 955 (1936).
[18] J. D. Ramshaw, Mol. Phys. **41**, 219 (1980).
[19] J. A. White and A. González, J. Phys. Condens. Matter **14**, 11907 (2002).